Optimal pulse sequences for population transfer in multilevel systems

Ignacio R. Solá,[1,2] Vladimir S. Malinovsky,[1,3,4] and David J. Tannor[1]
[1]*Chemical Physics Department, Weizmann Institute of Science, Rehovot 76100, Israel*
[2]*Departamento de Quimica Fisica, Universidad Complutense, 28040 Madrid, Spain*
[3]*Institute of Thermophysics, Russian Academy of Sciences, 630090 Novosibirsk, Russia*
[4]*Fachbereich Physik der Universität, 67653 Kaiserslautern, Germany*
(Received 8 September 1998; revised manuscript received 21 April 1999)

We study different mechanisms of adiabatic population transfer in *N*-level systems by means of optimal control algorithms. Using two-dimensional topographic maps of the yield of population transfer as a function of time delay and intensity of the pulses we analyze the global properties of the schemes and the conditions that lead to optimization. For three-level systems it is shown that the optimal pulse sequence is the well-known STIRAP (stimulated Raman adiabatic passage) scheme. For five-level systems a family of solutions ranging from the alternating STIRAP scheme to the new straddling STIRAP (S-STIRAP) scheme is obtained and the behavior of the solutions is compared. For four-level systems we obtain as optimal a S-STIRAP type sequence that behaves as an effective two-level system. For both odd and even numbers of *N*-level systems, the crucial role of the straddling pulse in reducing the population of all intermediate levels is demonstrated. [S1050-2947(99)04509-6]

PACS number(s): 32.80.Qk, 42.50.Hz, 33.80.Be

I. INTRODUCTION

Coherent population transfer by stimulated Raman adiabatic passage (STIRAP) has been an intense subject of research in recent years. This great interest derives both from the utility of being able to transfer population completely and robustly in multilevel quantum systems, as well as from the very intriguing counterintuitive pulse sequence employed in the scenario [1]. Indeed, the most striking feature of the STIRAP scenario is that the pump pulse, driving the transition between the initially populated level $|1\rangle$ and intermediate level $|2\rangle$, comes *after* the Stokes pulse, which drives the transition between the initially unpopulated levels $|2\rangle$ and $|3\rangle$. This ordering of pulses is both efficient and robust in achieving complete population transfer from state $|1\rangle$ to $|3\rangle$, while maintaining the population of state $|2\rangle$ at almost zero. The complete and robust transfer of population is relevant to many applications, including spectroscopy, collision dynamics, and optical control of chemical reactions. Specifically, we note the application of the STIRAP mechanism to atomic interferometry [2] and atomic cooling based on velocity-selective momentum transfer [3].

While for three-level systems the features of adiabatic passage have been thoroughly studied, attempts to devise equivalent strategies for general *N*-level systems have been less successful. Partially this situation can be attributed to the limitations of the analytic tools, based on the dressed-state picture, which are generally employed to determine the ''optimal'' pulse sequences. For Hamiltonians of even moderate complexity it is often no longer possible to find trapped states analytically. Moreover, several ''optimal'' scenarios may coexist. Very recently, however, two strategies have been proposed. The first one was restricted to sequentially coupled systems with an odd number of levels, involving a pulse sequence which we call the alternating STIRAP (A-STIRAP) scheme, where all the pulses corresponding to all even transitions precede all the pulses corresponding to all odd transitions [4]. The second one, which we call the straddling STIRAP (S-STIRAP) scheme, was proposed for any kind of sequentially coupled *N*-level system and involves a counterintuitive sequence of partially overlapping Stokes and pump pulses, *straddled* by pulses on resonance with all intermediate transitions [5].

Although the dressed-state picture is still a useful frame of reference for understanding the adiabatic passage processes, in this article we propose the use of optimal control theory (OCT) algorithms to obtain numerical solutions of the population transfer problem in order to ''guide the intuition.'' We show how different proposed schemes can be found by OCT and we further explore both analytically and numerically the behavior of the optimal sequences obtained. In recent years, the powerful tools of OCT have been applied successfully to a broad variety of physical and chemical systems [6,7]. But it has been argued on physical grounds that the STIRAP mechanism, where highly intense pulses are required, cannot be obtained from the general OCT equations (global control), where the fluency of energy in the pulses is either constrained or penalized. Indeed, a proof has been given demonstrating that the counterintuitive pulse sequence of STIRAP cannot be obtained within the usual framework of OCT [8]. Despite this prognosis, there is some preliminary evidence that STIRAP type solutions can emerge from global OCT equations [9]. Moreover, STIRAP solutions have been obtained from a variant of optimal control called ''local control,'' where the objective is optimized at each instant in time but laser fluency is unrestricted [5].

In this article we show the conditions for the counterintuitive STIRAP type solutions to emerge automatically from global optimal control equations. This is shown by means of a topographic map of the yield of population transfer as a simultaneous function of time delay and Rabi frequency. This map shows both the global properties of the population transfer caused by the given (parametrized) pulse sequence and the initial parameters that lead to the desired solution

through the gradients of the map. Using a penalty function on the population of the intermediate states and (if required) on the intensity of a set of pulses, the OCT algorithm can avoid the majority of the local maxima that appear in the complex topology and therefore allows one to find the area of adiabatic transfer. For a three-level system we show under what conditions we can find the STIRAP type solution. For five-level systems we study the contour plot of the yield of population transfer according to the S-STIRAP and the A-STIRAP schemes. We analyze the properties of the transfer as a function of other parameters, like the intensity of the intermediate pulses and the time delay between them, and we show that both schemes can be obtained by OCT depending on the election of penalties for the intermediate level population. Finally for four-level systems we show the same kind of analysis and we find that OCT can also be used to obtain the S-STIRAP scheme, although in this case the global behavior of the solution does not exhibit the adiabatic properties but instead it behaves as an effective two-level system.

In Sec. II, we present the general formalism of OCT applied to the coherent population transfer in *N*-level systems. In Sec. III, we apply the formalism to a three-level system and we show numerical solutions of the OCT equations of the STIRAP type and the domain of initial guesses that lead to them. The application of OCT to four- and five-level systems is presented in Sec. IV. In Sec. V we study the global properties of the solutions found for four- and five-level systems by means of simple analytic models. Section VI is the Conclusion.

II. GENERAL EQUATIONS

In this section we derive the set of coupled equations for the electromagnetic fields which optimize the coherent population transfer in an *N*-level system.

In the interaction representation and the rotating-wave approximation, the Schrödinger equation takes the form

$$i\dot{a}_i(t)=H_{ij}a_j(t), \tag{1}$$

where H_{ij} is the Hamiltonian, which is a function of the electromagnetic fields or corresponding Rabi frequencies, Ω_n, $a_i(t)$ is a vector of the probability amplitudes, and we set $\hbar=1$.

Optimal control theory starts by setting up an objective functional which depends on some expectation value of the system. In our case we would like to maximize a target state population $a_k^*(T)a_k(T)$ at final time T and minimize a functional of the trajectory, $L(T)=\int_0^T dt\, l(t)$, where $l(t)=l(\{a_i\},\{\Omega_n\},t)$ represents population in the unwanted intermediate levels. We can furthermore try to minimize the energy fluency of the fields, $\Upsilon(T)=\Sigma_n\int_0^T dt\,\Omega_n^2(t)$. This leads to a functional of the form

$$J=a_k^*(T)a_k(T)-\theta L(T)-\lambda\Upsilon(T), \tag{2}$$

where θ and λ are penalty parameters that can be functions of time.

Mathematically, we have to find optimal functions which maximize the objective functional [Eq. (2)]. In order to solve this problem we introduce a Lagrange multiplier vector b_j and the unconstrained functional

$$\overline{J}=J-\int_0^T dt\{b_i^*(t)[i\dot{a}_i^*(t)-H_{ij}(\{\Omega_n(t)\})a_j(t)]+\text{c.c}\}, \tag{3}$$

where c.c. denotes the complex conjugate.

Integrating by parts and taking derivatives of each of the unconstrained variables we get the following conditions for an extremum:

$$\frac{\delta\overline{J}}{\delta a_i^*(T)}=0\Rightarrow b_i(T)=a_i(T)\,\delta_{ik}, \tag{4}$$

$$\frac{\delta\overline{J}}{\delta a_i^*(t)}=0\Rightarrow i\dot{b}_i(t)=H_{ij}b_j(t)+\theta\frac{\partial l(t)}{\partial a_i^*(t)}, \tag{5}$$

$$\frac{\delta\overline{J}}{\delta\Omega_n(t)}=0\Rightarrow\Omega_n(t)=\frac{1}{2\lambda}\left[2\,\mathrm{Im}\left\{b_i^*(t)\frac{\partial H_{ij}}{\partial\Omega_n(t)}a_j(t)\right\}+\frac{\partial l(t)}{\partial\Omega_n(t)}\right]. \tag{6}$$

The solution to this set of equations allows one to find the optimal fields $\Omega_n(t)$ which maximize the target state population at final time.

III. OPTIMAL CONTROL OF THE COHERENT POPULATION TRANSFER IN THREE-LEVEL SYSTEMS

We now restrict attention to a three-level Λ system. We assume that there are two pulses, one which is resonant with the transition $|1\rangle\rightarrow|2\rangle$ (pump pulse) and the other which is resonant with the transition $|2\rangle\rightarrow|3\rangle$ (Stokes pulse):

$$E=E_p(t)\cos\omega_p t+E_s(t)\cos\omega_s t, \tag{7}$$

where $E_p(t)$ and $E_p(t)$ are the envelopes of the pulses. In the interaction representation and the rotating-wave approximation, the Schrödinger equation takes the form

$$\begin{pmatrix}\dot{a}_1(t)\\ \dot{a}_2(t)\\ \dot{a}_3(t)\end{pmatrix}=\frac{1}{2}\begin{pmatrix}0 & i\Omega_p(t)\exp\{i\Delta\omega_{21}t\} & 0\\ i\Omega_p(t)\exp\{-i\Delta\omega_{21}t\} & 0 & i\Omega_s(t)\exp\{-i\Delta\omega_{23}t\}\\ 0 & i\Omega_s(t)\exp\{i\Delta\omega_{23}t\} & 0\end{pmatrix}\begin{pmatrix}a_1(t)\\ a_2(t)\\ a_3(t)\end{pmatrix}, \tag{8}$$

where a_1, a_2, and a_3 are the probability amplitudes of the states $|1\rangle$, $|2\rangle$, and $|3\rangle$, $\Omega_p(t)=\mu_{12}E_p(t)/\hbar$ and $\Omega_s(t)=\mu_{23}E_s(t)/\hbar$ are the pump and Stokes Rabi frequencies, respectively, and $\Delta\omega_{21}=\omega_p-\omega_{21}$ and $\Delta\omega_{23}=\omega_s-\omega_{23}$ are the detunings of the laser frequencies $\omega_{p,s}$ from the transition frequencies $\omega_{21,23}$.

In the assumption of one-photon resonance ($\Delta\omega_{21}=\Delta\omega_{23}=0$), one can rewrite the Schrödinger equation in the following form:

$$\begin{pmatrix} \dot{a}_1(t) \\ \dot{a}_2(t) \\ \dot{a}_3(t) \end{pmatrix} = \frac{1}{2}\begin{pmatrix} 0 & i\Omega_p(t) & 0 \\ i\Omega_p(t) & 0 & i\Omega_s(t) \\ 0 & i\Omega_s(t) & 0 \end{pmatrix}\begin{pmatrix} a_1(t) \\ a_2(t) \\ a_3(t) \end{pmatrix}. \tag{9}$$

The objective is to maximize the population transferred to level $|3\rangle$ at final time T. At the same time, we try to minimize the population of the second level integrated over the entire process. Therefore we choose, as a functional of the trajectory, $l=a_2^*(t)a_2(t)$.

Equation (4) therefore takes the form $b_i(T)=a_i(T)\delta_{i3}$. Since l does not depend on $\Omega_{p,s}$, we find that

$$\frac{\delta l}{\delta a_i^*}=a_i^*(t)\delta_{i2}.$$

Equation (5) then takes the form

$$\begin{pmatrix} \dot{b}_1(t) \\ \dot{b}_2(t) \\ \dot{b}_3(t) \end{pmatrix} = \frac{1}{2}\begin{pmatrix} 0 & i\Omega_p(t) & 0 \\ i\Omega_p(t) & 0 & i\Omega_s(t) \\ 0 & i\Omega_s(t) & 0 \end{pmatrix}\begin{pmatrix} b_1(t) \\ b_2(t) \\ b_3(t) \end{pmatrix} + \begin{pmatrix} 0 \\ \theta a_2(t) \\ 0 \end{pmatrix}. \tag{10}$$

Finally, by taking variations of $\overline{J}$ with respect to $\Omega_{p,s}$ we obtain

$$\frac{\partial\overline{J}}{\partial\Omega_p}=-\mathrm{Im}[b_1^*(t)a_2(t)+b_2^*(t)a_1(t)]-\frac{1}{2}\lambda\Omega_p, \tag{11}$$

$$\frac{\partial\overline{J}}{\partial\Omega_s}=-\mathrm{Im}[b_2^*(t)a_3(t)+b_3^*(t)a_2(t)]-\frac{1}{2}\lambda\Omega_s. \tag{12}$$

Instead of using these equations to obtain closed forms for the optimal fields, we treat them as derivatives of the fields and we employ a gradient method to find the optimal fields. In doing so, we can solve the case of $\lambda=0$ (no restrictions in the energy fluency) using the usual gradient methodology and avoid the singularity in the equations for the optimal fields [compare with Eq. (6)].

We now show that this set of optimal control equations, when implemented numerically for the transfer of population in the three-level system, gives the counterintuitive solution of STIRAP, that is, the sequence of the Stokes pulse preceding the pump pulse.

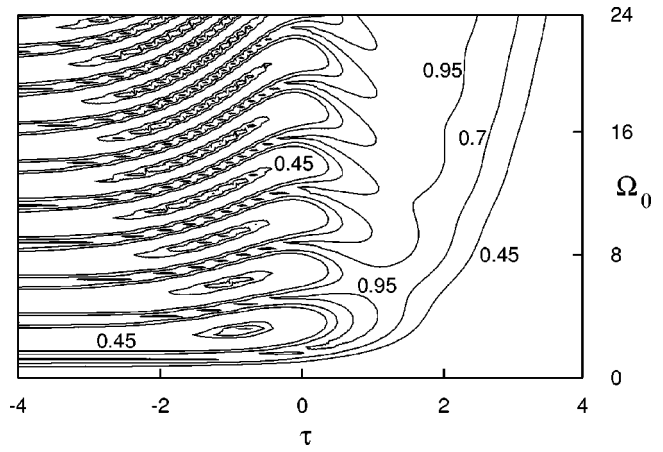

FIG. 1. Population transfer in a Λ system as a function of maximum Rabi frequency Ω_0 and time delay between the pump and Stokes pulses. The pump and Stokes pulses are here constrained to have the same shape and intensity. Positive delay implies that the Stokes precedes the pump pulse. The isolines represent final yields of 0.45, 0.70, and 0.95 in level $|3\rangle$. In the left part of the figure are the intuitively ordered solutions; the yield in this region is seen to be highly dependent on Ω_0. In the right part of the figure are the counterintuitive solutions, which provide almost complete population transfer over a broad set of values of Ω_0 and τ.

Figure 1 shows the population in state $|3\rangle$ at a final time T as a function of the Rabi frequencies and of the time delay between the pulses. To minimize the number of parameters, we have chosen pulse shapes of the form

$$\Omega_{p,s}(t)=\Omega_0/\cosh^2\left(t-\frac{T\pm\tau}{2}\right), \tag{13}$$

where Ω_0 is the maximum Rabi frequency, T is the final time, and τ is the time delay between the pulses. We have checked that the results are insensitive to the precise envelope of the pulses. The isolines in the plot represent final yields of 0.45, 0.70, and 0.95.

In the left part of the plot (negative delay, which in our notation implies that the pump pulse precedes the Stokes pulse) we can see the ''intuitive'' solutions. In the nonoverlapping case ($\tau\leqslant -4$), the maximum probability is obtained for pulse areas which are multiples of π, which reflects the strong dependence on the Rabi frequency. For overlapping conditions there appear ''islands'' of maximum probability for different pulse areas. In contrast, on the right side of the plot (positive delay) we can see an almost continuous area of maximum probability, reflecting the robustness of the counterintuitive solution. Since the probability in the plot is the value of our functional J, as defined in Sec. II (i.e., taking $\theta=0$), if we reduce the optimization search to the space of two parameters τ and Ω_0, the optimal control recipe is nothing more than an algorithm to find the maxima on the plot, following the gradient direction from each initial point. Therefore, from inspection of the plot we can anticipate which initial conditions lead to the counterintuitive solutions and which not.

As discussed in Sec. II, the OCT equations can be adjoined with a penalty function that penalizes the population in the second level. Such a penalty changes the landscape of

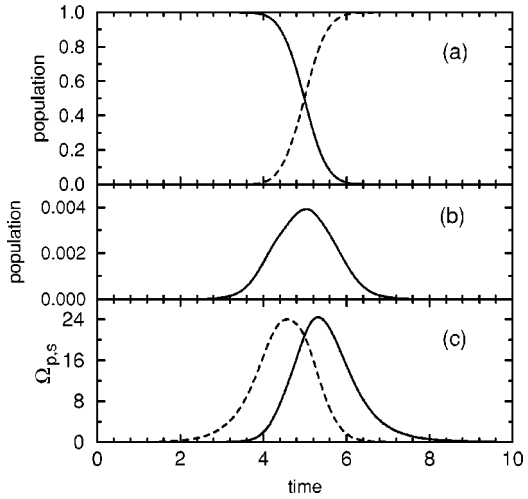

FIG. 2. Population transfer in a Λ system using global optimization. (a) The population of $|1\rangle$ (solid line) and $|3\rangle$ (dashed line). (b) Population of the intermediate level $|2\rangle$ vs time (note the difference in vertical scales). (c) The sequence of two optimal pulses found using the global optimization method. Note that the counterintuitive sequence of Stokes pulse (dashed line) followed by pump pulse (solid line) emerges automatically in the method.

the functional J and therefore the gradients that drive the search to the maximum yield. With a proper choice of the penalty for the time-dependent term θ, we actually remove almost all the ''intuitive'' solutions and therefore we increase the area of initial conditions which lead to the STIRAP solution. On the other hand, by changing the value of the penalty for the intensity of the fields, λ, we reduce the value of the functional for higher Ω_0 and therefore we remove the solutions in the upper part of the plot.

The drawback of the gradient approach is its difficulty in dealing with the complex topology of the functional in the rolling hills region, since for increasing values of Ω_0 there is a sequence of maxima and saddle points that prevent the method from finding the global maximum. (In Fig. 1 we can see only the first and most pronounced saddle point.) In contrast, the local control method [5] finds the global maximum directly, since it explicitly maintains low population in level $|2\rangle$. Nevertheless, we have found that by giving the OCT algorithm the freedom to change the shape of the pulses, instead of limiting the optimization to a reduced set of parameters, the gradient method finds eventually an optimal pulse close to the STIRAP solution. Figure 2 shows the optimum pulses and the associated dynamics, resulting from such an unrestricted optimization. The initial guess pulse has parameters $\Omega_{p,s}=10$ and $\tau=0$. We have tested the robustness of the scheme and have found that the penalty θ can be varied within 3 orders of magnitude without changing the final results significantly. If one starts from the intuitive order of the pulses ($\tau<0$), the unrestricted optimization procedure still finds the counterintuitive sequence, but the shapes of the optimal pulses obtained differ slightly from before.

IV. OPTIMAL CONTROL OF THE STIRAP MECHANISM IN FOUR- AND FIVE-LEVEL SYSTEMS

In a manner similar to our treatment of three-level systems, we can obtain generalized STIRAP pulse sequences from OCT for more complicated systems. In this section we restrict our analysis to the case of four- and five-level systems.

A. Five-level system

We consider first the five-level system, which is a prototype of multiple-level systems with an odd number of levels. For this case, several schemes which generalize the three-level STIRAP solution have been proposed. In one such scheme (A-STIRAP), all pulses have the same shape and intensity, but the pulses corresponding to all even transitions precede the pulses corresponding to all odd transitions [4]. In a second scheme (S-STIRAP) [5], the Stokes pulse again precedes the pump pulse, but now all the pulses connecting intermediate levels ''straddle'' both the Stokes and the pump pulses. Here we show that depending on the initial conditions and the parameters of optimization, the optimal control algorithm can find one scheme or the other.

We begin, as in the three-level scheme, by examining the global behavior of population transfer as a function of the pulse parameters. For this reason we consider pulses of the form

$$\Omega_{p,s}(t)=\Omega_0/\cosh^2\left(t-\frac{T\pm\tau}{2}\right) \tag{14}$$

[as in Eq. (13)] for the pump and Stokes pulses and

$$\Omega_{st_{1,2}}(t)=R_\Omega\Omega_0/\cosh^2\left(t-\frac{T\mp\tau_s}{2}\right) \tag{15}$$

for the intermediate pulses, where R_Ω is the ratio between the Rabi frequencies of the straddling and the pump-Stokes pulses and τ_s is the time delay between the straddling pulses defined positive if the first straddling pulse precedes the second one. With these choices the optimization is reduced to four parameters which allow the method to find either the S-STIRAP scheme ($R_\Omega>1,\tau_s\approx 0$) or the A-STIRAP scheme ($R_\Omega\approx 1,\tau_s>0$).

To analyze the global properties of the S-STIRAP scheme we show in Fig. 3 a topographic map of the yield of population transfer to the final state, $|5\rangle$, as a function of the time delay τ between the pump and Stokes pulses and of the effective Rabi frequency Ω_0. At the same time we keep fixed the ratio between the straddling and the pump-Stokes Rabi frequencies, $R_\Omega=3$, anticipating the result obtained by optimal control (to be shown below), and we set $\tau_s=0$. The solid contour lines in the plot represent final yields of 0.3, 0.6, and 0.9. Additionally we have plotted a dashed contour line enclosing those pulse conditions that lead to small population in the second level during all time. For the dashed line, the average population in the intermediate levels is less than or around 6%. Here the average population of the intermediate levels is defined by

$$\frac{1}{N}\sum_i^N \int dt P_i(t),$$

where N is the number of intermediate levels, $P_i(t)$ are the populations, and the time t is normalized by the width of the pulses.

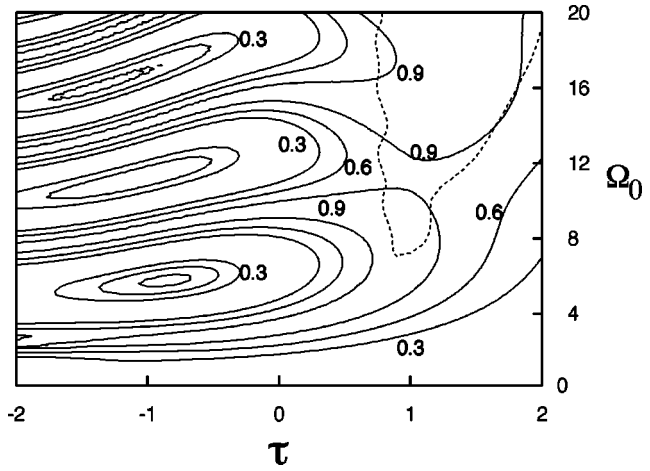

FIG. 3. Population transfer in a five-level, sequentially coupled system, as a function of time delay between the pump and Stokes pulses and effective Rabi frequency (Ω_0). Illustration of the S-STIRAP scheme. The ratio between the maximum Rabi frequency of the straddling pulses and the pump-Stokes pulses, R_Ω, is fixed at 3. The pump and Stokes pulses have the same shape and intensity, but we have made the straddling pulses broader so that the essential features of the method are easier to visualize. Positive delay implies that the Stokes precedes the pump pulse. The solid isolines represent final yields of 0.3, 0.6, and 0.9 population transfer. The dashed isoline represents an average population transfer of around 6% to the intermediate levels. The population transfer does not depend on R_Ω once the adiabatic regime is achieved.

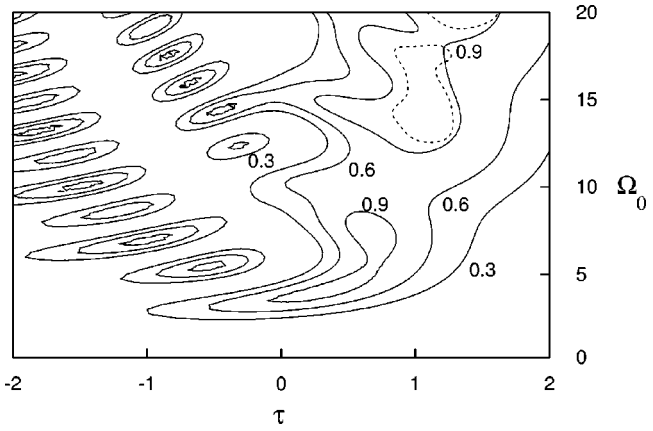

FIG. 4. Population transfer in a five-level, sequentially coupled system, as a function of time delay between the pulses, τ, and of the maximum Rabi frequency of the pulses, Ω_0. The figure corresponds to the solutions obtained by the A-STIRAP scheme. All pulses have the same shape and intensity. Positive delay implies that the pulses corresponding to all even transitions precede the pulses corresponding to all odd transitions. The solid isolines represent final yields of 0.3, 0.6, and 0.9 population transfer. The dashed isoline represents an average population transfer of about 12% to the intermediate levels.

From the plot we can observe the robustness of the S-STIRAP scheme in the counterintuitive region, which closely resembles the behavior of the STIRAP scheme for three-level systems. We quantify in the next section the properties of the solution based on a simple analytic model.

To analyze the global properties of the A-STIRAP scheme, we show in Fig. 4 the population in level $|5\rangle$ as a function of Rabi frequency Ω_0 and the time delay between even and odd pulses. In this case, $R_\Omega=1$ and $\tau_s=\tau$ so that the model is restricted to only two free parameters. The solid isolines represent final yields of 0.3, 0.6, and 0.9 but in this case the dashed isoline encloses pulse conditions that lead to less than or around 12% average population in the intermediate levels. The contribution to the population in the intermediate levels is not democratic, and it can easily be proved that although the population of the odd levels behaves exactly as in the S-STIRAP case, the A-STIRAP scheme *always* implies a significant transfer of population to level $|3\rangle$ (around 33% at intermediate times) in contrast with the S-STIRAP scheme. Moreover, the sensibility of the A-STIRAP scheme to the pulse parameters is also higher than that of the S-STIRAP scheme.

The OCT routines can provide both types of solutions depending on the election of the initial conditions and the set of penalties chosen. If we penalize the population of *all* intermediate levels, we obtain the S-STIRAP solution. We have performed an optimization of pulses of the form given by Eqs. (14) and (15) with initial parameters $\Omega_0=8$, $\tau=0$, $R_\Omega=1$, and $\tau_s=0$. The optimal sequence obtained, together with the population histories, is shown in Fig. 5. The results exhibit the main features of the S-STIRAP scheme. The intermediate pulses are about 3 times more intense than the pump-Stokes pulses, whose sequence is again counterintuitive. Note, in addition, that the second straddling pulse (connecting levels $|3\rangle$ and $|4\rangle$) slightly precedes the first straddling pulse, which connects levels $|2\rangle$ and $|3\rangle$. This last fact

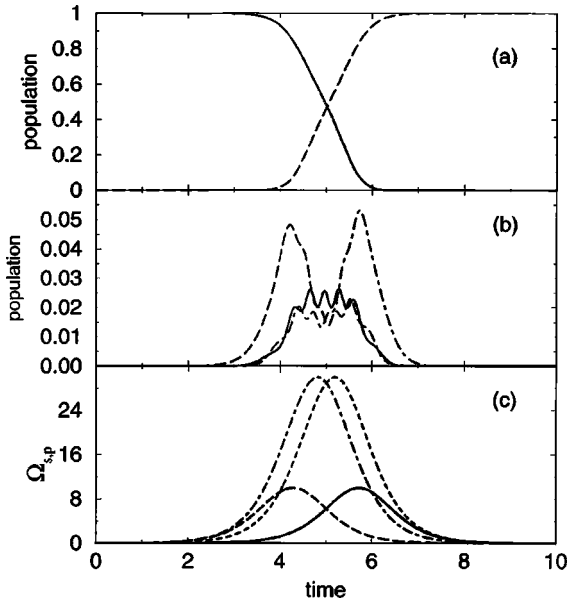

FIG. 5. Optimal results of population transfer in five-level, sequentially coupled system, corresponding to the S-STIRAP scheme. (a) The population of $|1\rangle$ (solid line) and $|5\rangle$ (dashed line) vs time. (b) The population of the intermediate levels $|2\rangle$ (dashed line), $|3\rangle$ (solid line), and $|4\rangle$ (dot-dashed line) vs time. (c) Optimal pulses. The counterintuitive sequence of Stokes pulse (dashed line) followed by pump pulse (solid line) again emerges automatically. However, now there are two additional pulses, resonant with the $|2\rangle\rightarrow|3\rangle$ (dotted line) and $|3\rangle\rightarrow|4\rangle$ (dot-dashed line) transition, not exactly overlapping, which envelop the Stokes and pump pulses, and are about 3 times more intense.

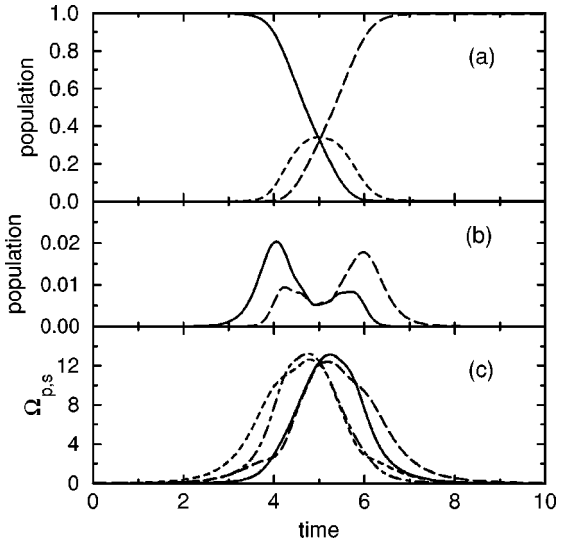

FIG. 6. Optimal results of population transfer in five-level, sequentially coupled system, corresponding to the A-STIRAP scheme. (a) The population of $|1\rangle$ (solid line), $|3\rangle$ (dotted line), and $|5\rangle$ (dashed line) vs time. (b) The population of the intermediate levels $|2\rangle$ (solid line) and $|4\rangle$ (dashed line) vs time. (c) Optical pulses. The pulses connecting even transitions (dashed line for the $|2\rangle \rightarrow |3\rangle$ transition and dotted line for the $|4\rangle \rightarrow |5\rangle$ transition) are preceding the pulses connecting odd transitions (solid line for the $|1\rangle \rightarrow |2\rangle$ transition and dot-dashed line for the $|3\rangle \rightarrow |4\rangle$ transition) in agreement with the A-STIRAP scheme.

ensures that the first intermediate pulse in fact straddles the pump pulse, as well as that the second one straddles the Stokes pulse. For higher values of R_Ω or if the optimization is performed using a broader shape for the intermediate pulses, the parameter τ_s no longer affects the final result.

Although different optimal parameters emerge from different sets of initial conditions, the S-STIRAP type solution is the underlying optimal scheme for almost any kind of initial sequence.

In order to obtain the A-STIRAP mechanism from global optimization we need to penalize the population of the even-numbered levels, $|2\rangle$ and $|4\rangle$, *but not* the population of level $|3\rangle$. In Fig. 6 we show the result of the optimization starting from initial conditions $\Omega_0=12$, $\tau=0$, $R_\Omega=1$, and $\tau_s=0$. The optimal sequence obtained can be identified as belonging to the A-STIRAP type. Actually it is harder to find initial conditions that give rise to the A-STIRAP scheme. The optimal control algorithm normally obtains the S-STIRAP scheme or mixed strategies. The critical parameter which determines to which scheme the optimization is going to converge is R_Ω. For low values of R_Ω, τ_s is normally slightly negative in order to assure the straddling condition. Nevertheless, if R_Ω decreases below some critical value, the intermediate pulses do not straddle at all, and τ_s tends to be positive in order to allow the S-STIRAP scheme to converge into the A-STIRAP scheme. We also point out that a full optimization (which allows the algorithm to change the shape of the pulses) can be used to obtain both schemes, although in this case this extra freedom does not imply an improvement in the performance of the method.

B. Four-level system

We turn our attention now to the four-level system. Figure 7 shows the population of the final state, $|4\rangle$, as a function of

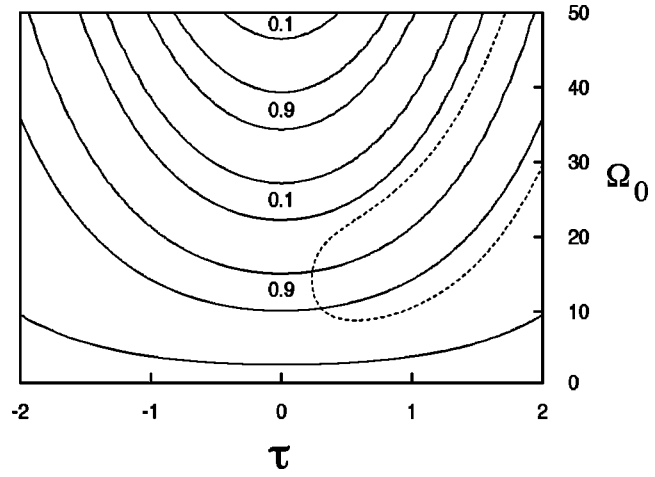

FIG. 7. Population transfer in a four-level, sequentially coupled system, as a function of the time delay between the pump and Stokes pulses and the effective Rabi frequency (Ω_0). We fix the ratio between the maximum Rabi frequency for the straddling pulse and the maximum Rabi frequency for the pump-Stokes pulse, $R_{\Omega_0}=6$. The pump and Stokes pulses have the same shape and intensity, but the straddling pulse is broader and overlaps both. Positive delay implies that the Stokes precedes the pump pulse. The solid isolines represent final yields of 0.1 and 0.9 population transfer. The dashed isoline represent an average population transfer of about 1% to the intermediate levels.

the time delay τ and of the effective Rabi frequency Ω_0 for fixed value of the ratio between the intermediate and the pump-Stokes Rabi frequencies, $R_\Omega=6$. In this case we change the form of the intermediate pulse,

$$\Omega_{st}(t)=R_\Omega\Omega_0/\cosh\left(t-\frac{T}{2}\right), \tag{16}$$

so that it is broader than the pump-Stokes pulses [Eq. (14)]. This different definition of the intermediate pulse facilitates its straddling character and makes easier the visualization and understanding of the symmetric properties of the solution, although the essential features are independent of the particular shape. The solid isolines represent yields of 0.1 and 0.9 population transfer. The dashed line again encloses conditions for the time average population in levels $|2\rangle$ and $|3\rangle$ less than or around 1%. The two main features of the solution are the symmetric behavior of the final population transfer (not the intermediate level population) with respect to time delay and its oscillatory behavior with respect to Rabi frequency. These oscillations, and the conditions for complete population transfer, are reminiscent of the behavior of a π pulse solution in two-level systems, where only the area of the pulse is important [10]. These properties are in stark contrast with those previously shown for the S-STIRAP scheme in five-level systems, and are analyzed in the next section.

It is also possible to obtain the S-STIRAP solution (as characterized by the counterintuitive sequence of pump-Stokes pulses and an intermediate straddling pulse) from OCT by penalizing the population in the intermediate levels. The results obtained after optimizing the set of parameters are shown in Fig. 8. In this figure we see that the intensity of

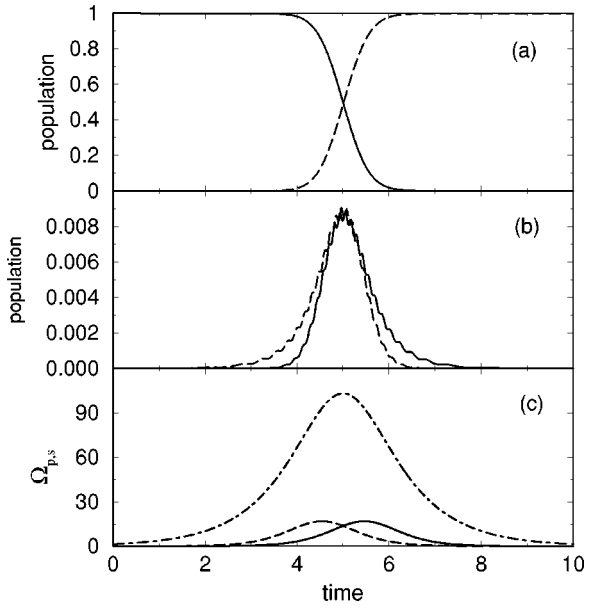

FIG. 8. Optimal results of population transfer in a four-level, sequentially coupled system. (a) The population of $|1\rangle$ (solid line) and $|4\rangle$ (dashed line) vs time. (b) Population of the intermediate levels $|2\rangle$ (solid line) and $|3\rangle$ (dashed line) vs time. (c) The sequence of optimal pulses. Note that the counterintuitive order of Stokes pulse (dashed line) and pump pulse (solid line) again emerges automatically. However, now there is a third pulse, the straddling pulse (dot-dashed line) resonant with the $|2\rangle \rightarrow |3\rangle$ transition, which envelops both these other pulses, and whose maximum Rabi frequency is about 6 times that of the other pulses.

the straddling pulse is about 6 times the intensity of the pump and Stokes pulses, leading to a maximum of about 1% population in both intermediate levels at the middle time of the pulses. Increasing the Rabi frequency of the straddle pulse decreases the population in the intermediate levels.

In closing this section we stress that although for both four- and five-level systems the pulse sequences that emerge from optimal control are not always easy to classify, the counterintuitive ordering of the pulses exciting the first and last transition *always* emerges from optimal control under appropriate choice of penalties.

V. EFFECTIVE THREE- AND TWO- LEVEL SYSTEMS

In this section we discuss the similarities and differences between the mechanisms at play in the optimal pulse sequences found above. Figures 1, 3, 4, and 7, which show the dependence of the population transfer on the pulse parameters, show significant differences between the different systems, particularly between the four-level system and the others. The optimal pulse corresponds, in each case, to a local maximum of the objective, and the flatness of the potential in the region of the maximum is a measure of the robustness of the solution, i.e., the stability with respect to changes in the pulse parameters. Inspection of Figs. 1, 3, and 4, for three- and five-level systems, indicates that the local maxima corresponding to counterintuitive pulse sequences lie in plateau regions, and therefore the population transfer is robust with respect to the parameters of the optimal pulse (effective Rabi frequency and time delay). However, Fig. 7, corresponding to a four-level system, shows a strong sensitivity to Rabi frequency, revealing the existence of a very different underlying physical mechanism. An analytical treatment of four- and five-level systems is now presented, which corroborated this significant difference in mechanisms.

A. Five-level system

It is clear from the comparison of Figs. 1, 3, and 4 that the population transfer in the five-level system (both by means of the S-STIRAP and the A-STIRAP schemes) shares some properties of the STIRAP scheme for three-level systems, namely, the counterintuitive sequence and the existence of a trapped state where the system is initially prepared. This means that in some sense the five level-system can be reduced to an effective three-level system. It turns out that there are in fact two different ways of doing this, the S-STIRAP and the A-STIRAP schemes, which give rise to different intermediate populations in level $|3\rangle$.

The five-level system Hamiltonian in the resonant case has the form

$$H(t)=-\frac{1}{2}\begin{pmatrix} 0 & \Omega_p(t) & 0 & 0 & 0 \\ \Omega_p(t) & 0 & \Omega_1(t) & 0 & 0 \\ 0 & \Omega_1(t) & 0 & \Omega_2(t) & 0 \\ 0 & 0 & \Omega_2(t) & 0 & \Omega_s \\ 0 & 0 & 0 & \Omega_s(t) & 0 \end{pmatrix}. \tag{17}$$

It is easy to find the eigenvalues of the Hamiltonian. For the case of the S-STIRAP pulse sequence ($\Omega_1=\Omega_2=\Omega_{ST}, \Omega_{ST} \gg \Omega_{p,s}$) the eigenvalues are

$$\lambda_0=0,$$

$$\lambda_{1,2}=\pm\frac{1}{2}\sqrt{(\Omega_s^2+\Omega_p^2)/2}, \tag{18}$$

$$\lambda_{3,4}=\pm\frac{1}{\sqrt{2}}\Omega_{ST}.$$

For the case of the A-STIRAP pulse sequence ($\Omega_1=\Omega_s, \Omega_2=\Omega_p$) they are

$$\lambda_0=0,$$

$$\lambda_{1,2}=\pm\frac{1}{2}\sqrt{\Omega_s^2+\Omega_p\Omega_s+\Omega_p^2}, \tag{19}$$

$$\lambda_{3,4}=\pm\frac{1}{2}\sqrt{\Omega_s^2-\Omega_p\Omega_s+\Omega_p^2}.$$

The eigenvector corresponding to λ_0 is, in the S-STIRAP case,

$$|c^0\rangle=\left\{\Omega_s;0;-\frac{\Omega_s\Omega_p}{\Omega_{ST}};0;\Omega_p\right\} \Big/ \Omega_e^s, \tag{20}$$

where $\Omega_e^s=\sqrt{\Omega_s^2+\Omega_p^2}$, whereas in the A-STIRAP case we have

$$|c^0\rangle = \{\Omega_s^2; 0; -\Omega_s\Omega_p; 0; \Omega_p^2\}/\Omega_e^a, \tag{21}$$

where $\Omega_e^a = \sqrt{\Omega_s^4 + \Omega_s^2\Omega_p^2 + \Omega_p^4}$.

It is clear that we have a dark state $|c^0\rangle$ which keeps the population only in levels $|1\rangle, |3\rangle$, and $|5\rangle$ in both cases. The difference resides, however, in the amplitude of probability in level $|3\rangle$ [Eqs. (19) and (20)].

Level $|3\rangle$ is most populated at the time (t_c) when the Rabi frequencies of the pump and Stokes pulses are equal. This maximum population is for the case of the A-STIRAP scheme, $P_3^{max} = 1/3$, in contrast with the S-STIRAP scheme where we have $P_3^{max} = \Omega_p^2(t=t_c)/2\Omega_{ST}^2(t=t_c)$. These values are represented in Fig. 6(a) and Fig. 5(b), respectively. This suggests a greater efficiency and robustness of the S-STIRAP scheme for the case where level $|3\rangle$ is not stable. As shown in the previous section, OCT is able to find both the A-STIRAP and the S-STIRAP pulse sequences depending on whether all intermediate level populations or only the even-numbered levels were penalized. In contrast, earlier studies using local control methodology found only the S-STIRAP scheme [5], because local optimization implies the locking of all intermediate level populations, therefore reducing the dimensionality of the Hamiltonian to that of an effective two-level system.

B. Four-level system

Although the general features of the optimal sequence obtained in Sec. IV, for a four-level system, superficially resemble those of the S-STIRAP solution for the five-level case, the topology of the solution as shown in Fig. 7 reveals a very different global behavior. Specifically, in Fig. 7 we do not observe any preference for the counterintuitive sequence, and the dependence of the final population transfer oscillates with respect to the effective Rabi frequency rather than following the adiabatic criteria $\Omega_e\tau_e \gg 1$. This implies a very different underlying mechanism of population transfer, which we now discuss.

The Hamiltonian for the four-level system in the resonant case is

$$H(t) = -\frac{1}{2}\begin{pmatrix} 0 & \Omega_p(t) & 0 & 0 \\ \Omega_p(t) & 0 & \Omega_{ST}(t) & 0 \\ 0 & \Omega_{ST}(t) & 0 & \Omega_s(t) \\ 0 & 0 & \Omega_s(t) & 0 \end{pmatrix}. \tag{22}$$

It is obvious that there is no $\lambda = 0$ eigenvalue for this Hamiltonian, which means that there cannot be found any dark or trapped state. The nature of the solution cannot be of STIRAP type as in the three- or five-level system. To show the properties of the solution we reduce the Hamiltonian to that of an effective two-level system. In order to do so, we make the transformation

$$a_i' = U a_i, \tag{23}$$

where

$$U = \begin{pmatrix} 1 & 0 & 0 & 0 \\ 0 & -\frac{1}{\sqrt{2}} & \frac{1}{\sqrt{2}} & 0 \\ 0 & \frac{1}{\sqrt{2}} & \frac{1}{\sqrt{2}} & 0 \\ 0 & 0 & 0 & 1 \end{pmatrix},$$

which leads to the following form of the Hamiltonian:

$$H'(t) = -\frac{1}{2}\begin{pmatrix} 0 & -\frac{1}{\sqrt{2}}\Omega_p(t) & \frac{1}{\sqrt{2}}\Omega_p(t) & 0 \\ -\frac{1}{\sqrt{2}}\Omega_p(t) & -\Omega_{ST}(t) & 0 & \frac{1}{\sqrt{2}}\Omega_s(t) \\ \frac{1}{\sqrt{2}}\Omega_p(t) & 0 & \Omega_{ST}(t) & \frac{1}{\sqrt{2}}\Omega_s(t) \\ 0 & \frac{1}{\sqrt{2}}\Omega_s(t) & \frac{1}{\sqrt{2}}\Omega_s(t) & 0 \end{pmatrix}. \tag{24}$$

Using the straddling condition, that is, $\Omega_{ST}(t) \gg \Omega_p(t), \Omega_s(t)$ all time, we apply the procedure of adiabatic elimination of the intermediate states a_2' and a_3'. It gives

$$a_2'(t) = -\frac{\Omega_p}{\sqrt{2}\Omega_{ST}}a_1(t) + \frac{\Omega_s}{\sqrt{2}\Omega_{ST}}a_4(t),$$

$$a_3'(t) = -\frac{\Omega_p}{\sqrt{2}\Omega_{ST}}a_1(t) - \frac{\Omega_s}{\sqrt{2}\Omega_{ST}}a_4(t).$$

Finally, we obtain the Schrödinger equation for an effective two-level system:

$$i\dot{a}_1(t) = \frac{\Omega_p \Omega_s}{2\Omega_{ST}} a_4(t), \tag{25}$$

$$i\dot{a}_4(t) = \frac{\Omega_p \Omega_s}{2\Omega_{ST}} a_1(t). \tag{26}$$

It is clear now that the solution of Eqs. (25) and (26) gives oscillations of the population transfer between levels $|1\rangle$ and $|4\rangle$ as a function of the effective Rabi frequency, $\Omega_e = \Omega_p \Omega_s / \Omega_{st}$. From the area theorem [10], we obtain the maxima of population transfer when the condition $\Omega_e \sim (2n+1)\pi/\tau$, with $n \geqslant 0$, is approximately accomplished. For fixed R_Ω this explains the sequence of equidistant maxima at $\Omega_0 \sim (2n+1)\pi R_\Omega / \tau$ that appears in Fig. 7.

It is also clear from the definition of Ω_e that in principle the population transfer is independent of the order of the pump and Stokes sequences. Nevertheless, in practice the intermediate level population can be further reduced if the Stokes pulse precedes the pump pulse. Finally, since Ω_e is clearly smaller than Ω_p and Ω_s, the scheme is more robust than the normal Rabi cycling for a three-level system, in the sense that only higher variations of Ω_p and Ω_s would imply a clear change in Ω_e and therefore the oscillation in the yield of the final transfer.

VI. CONCLUSIONS

We have derived general equations to obtain the optimal pulse sequences for population transfer in *N*-level systems. We have shown how some of the proposed adiabatic type pulse schemes can emerge within the framework of optimal control theory. By studying the global landscape portrait of the final-state population as a function of time delay and pulse intensity one obtains a clear understanding of which initial conditions lead to STIRAP type solutions and which do not. In defining the functional of the optimization we have found that it is important to impose an appropriate penalty function on the intermediate level populations, since restrictions on the intermediate level populations always favor a counterintuitive order in the optimal pulse sequence. In addition, the landscape portrait gives a good indication of the robustness of the scheme, as measured by the sensitivity of the final population to pulse parameter variation. The landscape portrait for a three-level system clearly shows that the STIRAP pulse sequence is the most robust solution. For five-level systems we find two different kinds of optimal sequences: the A-STIRAP and the S-STIRAP scheme, the last one more robust, restricting the population of *all* intermediate states. Both these schemes employ a dark state, analogous to the original STIRAP scheme in three-level systems. Finally, for four-level systems the S-STIRAP type sequence is again found to be optimal, although the global behavior exhibits the oscillatory properties of a two-level system.

In this paper we restricted our attention to the exact resonance conditions for sequentially coupled *N*-level systems. It is clear that allowing for a detuning of the carrier frequencies could have interesting effects, and indeed, some interesting results indicating that detuning can increase robustness in even *N*-level systems have been obtained in [11] and [12]. The possibility of applying OCT to population transfer in *N*-level systems with off-resonant excitation is currently under study.

ACKNOWLEDGMENTS

We thank Professor Klaas Bergmann, Professor Bruce Shore, and Dr. Nikolay Vitanov for stimulating discussions and for sending copies of their work prior to publication. I.R.S. gratefully acknowledges financial support from the Ministerio de Educacion y Ciencia (Spain) during his visit to the Weizmann Institute of Science. V.S.M. is grateful to the Deutsche Forschungsgemenschaft for support of his visit to Kaiserslautern during the final portions of this work. This work was supported by the U.S. Office of Naval Research and the the Israel Academy of Sciences (Mokad).

[1] K. Bergmann and B. W. Shore, in *Molecular Dynamics and Spectroscopy by Stimulated Emission Pumping*, edited by H. L. Dai and R. W. Field (World Scientific, Singapore, 1995); J.R. Kuklinski, U. Gaubatz, F.T. Hioe, and K. Bergmann, Phys. Rev. A **40**, 6741 (1989); T.A. Laine and S. Stenholm, *ibid.* **53**, 2501 (1996); J. Oreg, G. Hazak, and J.H. Eberly, *ibid.* **32**, 2776 (1985).

[2] P. Marte, P. Zoller, and J.L. Hall, Phys. Rev. A **44**, R4118 (1991); M. Weitz, B.C. Young, and S. Chu, Phys. Rev. Lett. **73**, 2563 (1994); P.D. Featonby, G.S. Summy, J.L. Martin, H. Wu, K.P. Zerie, C.J. Foot, and K. Burnett, Phys. Rev. A **53**, 373 (1996).

[3] J. Lawall, F. Bardou, B. Saubamea, K. Shimizu, M. Leduc, A. Aspect, and C. Cohen-Tannoudji, Phys. Rev. Lett. **73**, 1915 (1994); T. Esslinger, F. Sander, M. Weidemüller, A. Hemmerich, and T.W. Hänsch, *ibid.* **76**, 2432 (1996); S. Kulin, B. Saubamea, E. Peik, J. Lawall, T.W. Hijmans, M. Leduc, and C. Cohen-Tannoudji, *ibid.* **78**, 4185 (1997).

[4] B.W. Shore, K. Bergmann, J. Oreg, and S. Rosenwaks, Phys. Rev. A **44**, 7442 (1991).

[5] V.S. Malinovsky and D.J. Tannor, Phys. Rev. A **56**, 4929 (1997).

[6] W.S. Warren, H. Rabitz, and M. Dahleh, Science **259**, 1581 (1993); B. Kohler, J. Krause, F. Raksi, K.R. Wilson, R.M. Whitnell, V.V. Yakovlev, and Y. Yan, Acc. Chem. Res. **28**, 133 (1995); P. Brumer and M. Shapiro, Sci. Am. (Int. Ed.) **272** (3), 56 (1995); S.A. Rice, Adv. Chem. Phys. **101**, 213 (1997); R. Gordon and S.A. Rice, Annu. Rev. Phys. Chem. **48**, 595 (1997).

[7] D.J. Tannor and S.A. Rice, Adv. Chem. Phys. **70**, 441 (1988); R. Kosloff, S.A. Rice, P. Gaspard, S. Tersigni, and D.J. Tannor, Chem. Phys. **139**, 201 (1989); R. Kosloff, A.D. Hammerich, and D. Tannor, Phys. Rev. Lett. **69**, 2172 (1992); A. Bartana, R. Kosloff, and D.J. Tannor, J. Chem. Phys. **99**, 196

(1993); H. Tang, R. Kosloff, and S.A. Rice, *ibid.* **104**, 5457 (1996); V.S. Malinovsky, C. Meier, and D.J. Tannor, Chem. Phys. **221**, 67 (1997).
[8] Y.B. Band and O. Magnes, J. Chem. Phys. **101**, 7528 (1994).
[9] N. Wang and H. Rabitz, J. Chem. Phys. **104**, 1173 (1996).
[10] B. W. Shore, *The Theory of Coherent Atomic Excitation* (Wiley, New York, 1990).
[11] N.V. Vitanov, Phys. Rev. A **58**, 2295 (1998); N.V. Vitanov, B.W. Shore, and K. Bergmann, Eur. Phys. J D **4**, 15 (1998).
[12] T. Nakajima, Phys. Rev. A **59**, 559 (1999).